

# Model independent analysis of New Physics effects on $B_c \rightarrow (D_s, D_s^*) \mu^+ \mu^-$ decay observables

Rupak Dutta\*

National Institute of Technology Silchar, Silchar 788010, India

Motivated by the anomalies present in  $b \rightarrow s l^+ l^-$  neutral current decays, we study the corresponding  $B_c \rightarrow (D_s, D_s^*) \mu^+ \mu^-$  decays within the standard model and beyond. We use a model independent effective theory formalism in the presence of vector and axial vector new physics operators and study the implications of the latest global fit to the  $b \rightarrow s l^+ l^-$  data on various observables for the  $B_c \rightarrow (D_s, D_s^*) \mu^+ \mu^-$  decays. We give predictions on several observables such as the differential branching ratio, ratio of branching ratios, forward backward asymmetry, and the longitudinal polarization fraction of the  $D_s^*$  meson within standard model and within various new physics scenarios. These results can be tested at the Large Hadron Collider and, in principle, can provide complimentary information regarding new physics in  $b \rightarrow s l^+ l^-$  neutral current decays.

## I. INTRODUCTION

Although standard model (SM) of particle physics is successful in explaining various experimental observations, it, however, can not accommodate several long standing issues such as dark matter, dark energy, neutrino mass, matter antimatter asymmetry in the universe etc. It is indeed certain that physics beyond the SM exists. There are two ways to determine the nature of new physics (NP). One is direct detection of new particles and their interactions and another is indirect detection through their effects on various low energy processes. In this respect, flavor physics can, in principle, be the ideal platform to look for indirect evidences of NP. In fact, various anomalies with the SM prediction have been reported by dedicated experiments such as BABAR, Belle, and more recently by LHCb. In particular, measurement of various observables in  $b \rightarrow c \tau \nu$  charged current interactions and in  $b \rightarrow s l^+ l^-$  neutral current interactions already provided hints of NP. We will focus here on anomalies present in  $B$  meson decays mediated via  $b \rightarrow s l^+ l^-$  neutral current interactions. The most important observables are the lepton flavor universality (LFU) ratios  $R_K$  and  $R_{K^*}$ , various angular observables in  $B \rightarrow K^* \mu^+ \mu^-$  decays, and the branching ratio of  $B_s \rightarrow \phi \mu^+ \mu^-$  decays. The experimental results confirming these anomalies are listed below.

A significant deviation from the SM expectation is observed in the LFU ratios  $R_K$  and  $R_{K^*}$  defined as

$$R_K^{(*)} = \frac{\mathcal{B}(B \rightarrow K^{(*)} \mu \mu)}{\mathcal{B}(B \rightarrow K^{(*)} e e)}. \quad (1)$$

The first LHCb measurement of  $R_K = 0.745_{-0.074}^{+0.090} \pm 0.036$  [1] in the low  $q^2$  bin  $1 < q^2 < 6 \text{ GeV}^2$  deviates from the SM prediction  $R_K \approx 1$  [2–4] at  $2.6\sigma$  level. Very recently, the earlier measurement was superseded by LHCb Collaboration and it is reported to be  $R_K = 0.846_{-0.054-0.014}^{+0.060+0.016}$  [5]. Although it moves closer to the SM value, the deviation with the SM prediction still stands at  $2.5\sigma$  level. Similarly, the measured value of  $R_{K^*} = 0.66_{-0.07}^{+0.11} \pm 0.03$  and  $0.69_{-0.07}^{+0.11} \pm 0.05$  in the dilepton invariant mass  $q^2 = [0.045, 1.1] \text{ GeV}^2$  and  $[1.1, 6.0] \text{ GeV}^2$  [6] deviate from the SM prediction of  $R_{K^*} \approx 1$  [7, 8] at approximately  $2.1\sigma$  and  $2.4\sigma$ , respectively. Very recently, Belle collaboration has reported the values of  $R_{K^*}$  in multiple  $q^2$  bin but with a much larger uncertainties [9]. The other notable deviation is the deviation observed in the angular observable  $P'_5$  in  $B \rightarrow K^* \mu^+ \mu^-$  decays [10, 11]. LHCb [12, 13] and ATLAS [14] have measured the value of the angular observable  $P'_5$  in the  $q^2$  range  $4.0 < q^2 < 6.0 \text{ GeV}^2$  and the deviation from the SM prediction is found to be more than  $3\sigma$  [15]. Belle [16] and CMS [17] have also measured this observable in the  $q^2$  bin  $4.3 < q^2 < 8.68 \text{ GeV}^2$  and  $4.3 < q^2 < 6.0 \text{ GeV}^2$ , respectively. Although the Belle measured value differs from the SM expectation at  $2.6\sigma$  level, the measured value by CMS is consistent with the SM expectation at  $1\sigma$  level. Similarly, there is a systematic deficit in the measured value of branching ratio of  $B_s \rightarrow \phi \mu^+ \mu^-$  [18, 19] decays as compared to the SM prediction [15, 20]. Currently the deviation with the SM prediction stands at around  $3.7\sigma$ . If it persists and is confirmed by future experiments, it could unravel new flavor structure beyond the SM physics. Various

---

\*Electronic address: rupak@phy.nits.ac.in

global fits [21–30] to the  $b \rightarrow s l^+ l^-$  data have been performed and it was suggested that some of these anomalies can be resolved by modifying the Wilson coefficients (WCs).

If these anomalies are due to NP, this will show up in other  $b \rightarrow s l^+ l^-$  transition decays as well. In this paper, we analyze  $B_c \rightarrow (D_s, D_s^*) \mu^+ \mu^-$  decays mediated via  $b \rightarrow s l^+ l^-$  neutral current transitions within the SM and in several NP scenarios. LHCb has already measured the ratio of branching ratio  $R_{J/\Psi}$  in  $B_c \rightarrow J/\Psi l \nu$  decays. Detection and measurement of various observables pertaining to  $B_c$  meson decaying to other mesons via  $b \rightarrow s l^+ l^-$  neutral current interactions will be feasible once more and more data will be accumulated by LHCb. It is worth mentioning that the study of such modes is complimentary to the study of  $B \rightarrow (K, K^*) \mu^+ \mu^-$  decays and it can, in principle, provide useful information regarding different NP Lorentz structures. Moreover, study of these decay modes both theoretically and experimentally can act as a useful ingredient in maximizing future sensitivity to NP.

Within the SM,  $B_c \rightarrow (D_s, D_s^*) \mu^+ \mu^-$  decays have been studied previously using the relativistic constituent quark model [31], light-front quark model [32, 33], QCD sum rules [34, 35], and relativistic quark model [36]. In this paper, we use the relativistic quark model of Ref. [36] and supplement the previous analysis by analyzing the effect of various NP on these decay modes in a model independent way. We use an effective theory formalism in the presence of new vector and axial vector couplings that couples only to the muon sector. We give prediction of various observables such as the ratio of branching ratios, lepton side forward backward asymmetry, and the longitudinal polarization fraction of the  $D_s^*$  meson within the SM and within various NP scenarios.

Our paper is organized as follows. In section II, we start with the effective weak Hamiltonian for  $b \rightarrow s l^+ l^-$  decays in the presence of new vector and axial vector operators. We also discuss the hadronic matrix elements of  $B_c \rightarrow D_s$  and  $B_c \rightarrow D_s^*$  and their parametrization in terms of various meson to meson transition form factors. In section III, we write down the helicity amplitudes for the  $B_c \rightarrow D_s \mu^+ \mu^-$  and  $B_c \rightarrow D_s^* \mu^+ \mu^-$  decay modes and construct several observables. In section IV, we give predictions of all the observables in the SM and in several NP cases obtained from the global fit. We conclude with a brief summary of our results in section V.

## II. FORMALISM

The most general effective weak Hamiltonian in the presence of new vector and axial vector operators for the  $|\Delta B| = |\Delta S| = 1$  transition can be written as

$$\begin{aligned} \mathcal{H}_{\text{eff}} = & -\frac{4G_F}{\sqrt{2}} V_{tb} V_{ts}^* \frac{\alpha_e}{4\pi} \left[ C_9^{\text{eff}} \bar{s} \gamma^\mu P_L b \bar{l} \gamma_\mu l + C_{10} \bar{s} \gamma^\mu P_L b \bar{l} \gamma_\mu \gamma_5 l - \frac{2m_b}{q^2} C_7^{\text{eff}} \bar{s} i \not{q} \sigma^{\mu\nu} P_R b \bar{l} \gamma_\mu l \right. \\ & \left. + C_9^{NP} \bar{s} \gamma^\mu P_L b \bar{l} \gamma_\mu l + C_{10}^{NP} \bar{s} \gamma^\mu P_L b \bar{l} \gamma_\mu \gamma_5 l + C_9' \bar{s} \gamma^\mu P_R b \bar{l} \gamma_\mu l + C_{10}' \bar{s} \gamma^\mu P_R b \bar{l} \gamma_\mu \gamma_5 l \right], \end{aligned} \quad (2)$$

where  $G_F$  is the Fermi coupling constant,  $\alpha_e$  is the electromagnetic coupling constant,  $V_{tb}$  and  $V_{ts}$  are the relevant Cabibbo Kobayashi Maskawa (CKM) matrix elements, and  $P_{R,L} = (1 \pm \gamma_5)/2$  are the chiral projectors. All the WCs are evaluated at a renormalization scale of  $\mu = m_b^{\text{pole}} = 4.8 \text{ GeV}$ . The  $b$  quark mass associated with  $C_7^{\text{eff}}$  is considered to be running mass in the  $\overline{\text{MS}}$  scheme. In principle, there can be several NP Lorentz structures such as vector, axial vector, scalar, pseudoscalar, and tensor. The scalar, pseudoscalar and the tensor NP operators are severely constrained by  $B_s \rightarrow \mu\mu$  and  $b \rightarrow s\gamma$  measurements [37–39]. Hence, we consider NP in the form of vector and axial vector operators only. Again, we do not consider NP in the dipole operator as these are well constrained by radiative decays. The non factorizable corrections coming from electromagnetic corrections to the matrix elements of purely hadronic operators in the weak effective Hamiltonian are ignored in our analysis. These corrections, however, are expected to be significant at low  $q^2$  [40, 41]. All the NP WCs  $C_9^{NP}$ ,  $C_{10}^{NP}$ ,  $C_9'$ , and  $C_{10}'$  are assumed to be real for our analysis. In the SM,  $C_9^{NP} = C_{10}^{NP} = C_9' = C_{10}' = 0$ . The effective WCs  $C_7^{\text{eff}}$  and  $C_9^{\text{eff}}$  are defined as

$$\begin{aligned} C_7^{\text{eff}} &= C_7 - \frac{1}{3} C_5 - C_6, \\ C_9^{\text{eff}} &= C_9 + y(q^2) + y_{\text{BW}}(q^2), \end{aligned} \quad (3)$$

where the contributions coming from the one loop matrix elements of the four quark operators are contained in [42]

$$\begin{aligned} y(q^2) = & h\left(\frac{m_c}{m_b}, \frac{q^2}{m_b^2}\right) (3C_1 + C_2 + 3C_3 + C_4 + 3C_5 + C_6) - \frac{1}{2} h\left(1, \frac{q^2}{m_b^2}\right) (4C_3 + 4C_4 + 3C_5 + C_6) \\ & - \frac{1}{2} h\left(0, \frac{q^2}{m_b^2}\right) (C_3 + 3C_4) + \frac{2}{9} (3C_3 + C_4 + 3C_5 + C_6). \end{aligned} \quad (4)$$

Here

$$h(z, s) = -\ln \frac{m_b}{\mu} - \frac{8}{9} \ln z + \frac{8}{27} + \frac{4}{9}x - \frac{2}{9}(2+x)|1-x|^{1/2} \begin{cases} \ln \left| \frac{\sqrt{1-x}+1}{\sqrt{1-x}-1} \right| - i\pi & \text{for } x = \frac{4z^2}{s} < 1 \\ 2 \arctan \frac{1}{\sqrt{x-1}} & \text{for } x = \frac{4z^2}{s} > 1 \end{cases}$$

$$h(0, s) = \frac{8}{27} - \ln \frac{m_b}{\mu} - \frac{4}{9} \ln s + \frac{4}{9} i\pi. \quad (5)$$

The phenomenological parameter  $y_{BW}(q^2)$  involves the long distance effects coming from the  $c\bar{c}$  resonance contributions coming from  $J/\Psi$ ,  $\Psi'$  etc. In particular, these resonances provide large peaked contributions in the  $q^2$  bins that are close to these charmonium resonance masses. The corresponding  $q^2$  bins are not considered in our analysis. The values of masses of charm and bottom quark in these expressions are defined in pole mass scheme. The WCs that contains the short distance contribution can be calculated perturbatively, whereas, for the calculation of the long distance contributions contained in the matrix elements of local operators between initial and final hadron states, it requires non perturbative approach. The hadronic matrix elements can be expressed in terms of various meson to meson transition form factors.

The hadronic matrix elements for the  $B_c \rightarrow D_s \mu^+ \mu^-$  decays can be parametrized in terms of three invariant form factors. Those are

$$\begin{aligned} \langle D_s | \bar{s} \gamma^\mu b | B_c \rangle &= f_+(q^2) \left[ p_{B_c}^\mu + p_{D_s}^\mu - \frac{M_{B_c}^2 - M_{D_s}^2}{q^2} q^\mu \right] + f_0(q^2) \frac{M_{B_c}^2 - M_{D_s}^2}{q^2} q^\mu, \\ \langle D_s | \bar{s} \sigma^{\mu\nu} q_\nu b | B_c \rangle &= \frac{i f_T(q^2)}{M_{B_c} + M_{D_s}} \left[ q^2 (p_{B_c}^\mu + p_{D_s}^\mu - (M_{B_c}^2 - M_{D_s}^2) q^\mu) \right]. \end{aligned} \quad (6)$$

Similarly, for the  $B_c \rightarrow D_s^* \mu^+ \mu^-$  decays, the hadronic matrix elements can be parametrized in terms of seven invariant form factors, i.e.,

$$\begin{aligned} \langle D_s^* | \bar{s} \gamma^\mu b | B_c \rangle &= \frac{2iV(q^2)}{M_{B_c} + M_{D_s^*}} \epsilon^{\mu\nu\rho\sigma} \epsilon_\nu^* p_{B_c\rho} p_{D_s^*\sigma}, \\ \langle D_s^* | \bar{s} \gamma^\mu \gamma_5 b | B_c \rangle &= 2M_{D_s^*} A_0(q^2) \frac{\epsilon^* \cdot q}{q^2} q^\mu + (M_{B_c} + M_{D_s^*}) A_1(q^2) \left( \epsilon^{\mu*} - \frac{\epsilon^* \cdot q}{q^2} q^\mu \right) \\ &\quad - A_2(q^2) \frac{\epsilon^* \cdot q}{M_{B_c} + M_{D_s^*}} \left[ p_{B_c}^\mu + p_{D_s^*}^\mu - \frac{M_{B_c}^2 - M_{D_s^*}^2}{q^2} q^\mu \right], \\ \langle D_s^* | \bar{s} i \sigma^{\mu\nu} q_\nu b | B_c \rangle &= 2T_1(q^2) \epsilon^{\mu\nu\rho\sigma} \epsilon_\nu^* p_{B_c\rho} p_{D_s^*\sigma}, \\ \langle D_s^* | \bar{s} i \sigma^{\mu\nu} \gamma_5 q_\nu b | B_c \rangle &= T_2(q^2) \left[ (M_{B_c}^2 - M_{D_s^*}^2) \epsilon^{\mu*} - (\epsilon^* \cdot q) (p_{B_c}^\mu + p_{D_s^*}^\mu) \right] \\ &\quad + T_3(q^2) (\epsilon^* \cdot q) \left[ q^\mu - \frac{q^2}{M_{B_c}^2 - M_{D_s^*}^2} (p_{B_c}^\mu + p_{D_s^*}^\mu) \right], \end{aligned} \quad (7)$$

where  $q^\mu = (p_B - p_{D_s, D_s^*})^\mu$  is the four momentum transfer and  $\epsilon_\mu$  is polarization vector of the  $D_s^*$  meson. For the  $B_c \rightarrow D_s$  and  $B_c \rightarrow D_s^*$  transition form factors we follow the relativistic quark model adopted in Ref. [36]. It was mentioned in Ref. [36] that in the limit of infinitely heavy quark mass and large energy of the final meson, the form factor results obtained in this approach are consistent with all the model independent symmetry relations [43, 44]. We refer to Ref. [36] for all the omitted details.

### III. HELICITY AMPLITUDES AND DECAY OBSERVABLES

For the helicity amplitudes, we pattern our analysis after that of Ref. [36] and, indeed, adopt a common notation. We use the helicity techniques of Refs. [45, 46] and write the hadronic helicity amplitudes for  $B_c \rightarrow D_s l^+ l^-$  decays

in the presence of vector and axial vector NP operators as follows:

$$\begin{aligned}
H_{\pm}^{(i)} &= 0, \\
H_0^{(1)} &= \sqrt{\frac{\lambda}{q^2}} \left[ (C_9^{\text{eff}} + C_9^{NP} + C'_9) f_+(q^2) + C_7^{\text{eff}} \frac{2m_b}{M_{B_c} + M_{D_s}} f_T(q^2) \right] \\
H_0^{(2)} &= \sqrt{\frac{\lambda}{q^2}} (C_{10} + C_{10}^{NP} + C'_{10}) f_+(q^2), \\
H_t^{(1)} &= \frac{M_{B_c}^2 - M_{D_s}^2}{q^2} (C_9^{\text{eff}} + C_9^{NP} + C'_9) f_0(q^2), \\
H_t^{(2)} &= \frac{M_{B_c}^2 - M_{D_s}^2}{q^2} (C_{10} + C_{10}^{NP} + C'_{10}) f_0(q^2)
\end{aligned} \tag{8}$$

Similarly, for  $B_c \rightarrow D_s^* l^+ l^-$  decays, the hadronic helicity amplitudes are

$$\begin{aligned}
H_{\pm}^{(1)} &= -(M_{B_c}^2 - M_{D_s^*}^2) \left[ (C_9^{\text{eff}} + C_9^{NP} - C'_9) \frac{A_1(q^2)}{M_{B_c} - M_{D_s^*}} + \frac{2m_b}{q^2} C_7^{\text{eff}} T_2(q^2) \right] \\
&\quad \pm \sqrt{\lambda} \left[ (C_9^{\text{eff}} + C_9^{NP} + C'_9) \frac{V(q^2)}{M_{B_c} + M_{D_s^*}} + \frac{2m_b}{q^2} C_7^{\text{eff}} T_2(q^2) \right], \\
H_{\pm}^{(2)} &= (C_{10} + C_{10}^{NP} - C'_{10}) \left[ -(M_{B_c} + M_{D_s^*}) A_1(q^2) \right] \pm (C_{10} + C_{10}^{NP} + C'_{10}) \frac{\lambda}{M_{B_c} + M_{D_s^*}} V(q^2), \\
H_0^{(1)} &= -\frac{1}{2M_{D_s^*} \sqrt{q^2}} \left\{ (C_9^{\text{eff}} + C_9^{NP} - C'_9) \left[ (M_{B_c}^2 - M_{D_s^*}^2 - q^2) (M_{B_c} + M_{D_s^*}) A_1(q^2) - \frac{\lambda}{M_{B_c} + M_{D_s^*}} A_2(q^2) \right] \right. \\
&\quad \left. + 2m_b C_7^{\text{eff}} \left[ (M_{B_c}^2 + 3M_{D_s^*}^2 - q^2) T_2(q^2) - \frac{\lambda}{M_{B_c}^2 - M_{D_s^*}^2} T_3(q^2) \right] \right\} \\
H_0^{(2)} &= -\frac{1}{2M_{D_s^*} \sqrt{q^2}} (C_{10} + C_{10}^{NP} - C'_{10}) \left[ (M_{B_c}^2 - M_{D_s^*}^2 - q^2) (M_{B_c} + M_{D_s^*}) A_1(q^2) - \frac{\lambda}{M_{B_c} + M_{D_s^*}} A_2(q^2) \right] \\
H_t^{(1)} &= -\sqrt{\frac{\lambda}{q^2}} (C_9^{\text{eff}} + C_9^{NP} - C'_9) A_0(q^2), \\
H_t^{(2)} &= -\sqrt{\frac{\lambda}{q^2}} (C_{10} + C_{10}^{NP} - C'_{10}) A_0(q^2),
\end{aligned} \tag{9}$$

where

$$\lambda = M_{B_c}^4 + M_{D_s, D_s^*}^4 + q^4 - 2(M_{B_c}^2 M_{D_s, D_s^*}^2 + M_{D_s, D_s^*}^2 q^2 + M_{B_c}^2 q^2) \tag{10}$$

Using the helicity amplitudes, the three body  $B_c \rightarrow D_s l^+ l^-$  and  $B_c \rightarrow D_s^* l^+ l^-$  differential decay rate can be written as [36]

$$\begin{aligned}
\frac{d\Gamma}{dq^2} &= \frac{G_F^2}{(2\pi)^3} \left( \frac{\alpha_e |V_{tb} V_{ts}^*|}{2\pi} \right)^2 \frac{\lambda^{1/2} q^2}{48 M_{B_c}^3} \sqrt{1 - \frac{4m_l^2}{q^2}} \left[ H^{(1)} H^{\dagger(1)} \left( 1 + \frac{4m_l^2}{q^2} \right) + H^{(2)} H^{\dagger(2)} \left( 1 - \frac{4m_l^2}{q^2} \right) \right. \\
&\quad \left. + \frac{2m_l^2}{q^2} 3 H_t^{(2)} H_t^{\dagger(2)} \right],
\end{aligned} \tag{11}$$

where  $m_l$  denotes the mass of lepton and

$$H^{(i)} H^{\dagger(i)} = H_+^{(i)} H_+^{\dagger(i)} + H_-^{(i)} H_-^{\dagger(i)} + H_0^{(i)} H_0^{\dagger(i)}. \tag{12}$$

We define the differential ratio of branching ratio as follows:

$$R_{D_s, D_s^*}(q^2) = \frac{d\Gamma/dq^2(B_c \rightarrow (D_s, D_s^*) \mu^+ \mu^-)}{d\Gamma/dq^2(B_c \rightarrow (D_s, D_s^*) e^+ e^-)}. \tag{13}$$

We also construct observables like the forward backward asymmetry of the lepton pair  $A_{FB}$  and the longitudinal polarization fraction of the  $D_s^*$  meson  $F_L$  as a function of dilepton invariant mass  $q^2$ . The forward backward asymmetry  $A_{FB}(q^2)$  is given by [36]

$$A_{FB}(q^2) = \frac{3}{4} \sqrt{1 - \frac{4m_l^2}{q^2}} \left\{ \frac{\text{Re}(H_+^{(1)} H_+^{\dagger(2)}) - \text{Re}(H_-^{(1)} H_-^{\dagger(2)})}{H^{(1)} H^{\dagger(1)} \left(1 + \frac{4m_l^2}{q^2}\right) + H^{(2)} H^{\dagger(2)} \left(1 - \frac{4m_l^2}{q^2}\right) + \frac{2m_l^2}{q^2} 3 H_t^{(2)} H_t^{\dagger(2)}} \right\}. \quad (14)$$

Similarly, the longitudinal polarization fraction of the  $D_s^*$  meson can be written as [36]

$$F_L(q^2) = \frac{H_0^{(1)} H_0^{\dagger(1)} \left(1 + \frac{4m_l^2}{q^2}\right) + H_0^{(2)} H_0^{\dagger(2)} \left(1 - \frac{4m_l^2}{q^2}\right) + \frac{2m_l^2}{q^2} 3 H_t^{(2)} H_t^{\dagger(2)}}{H^{(1)} H^{\dagger(1)} \left(1 + \frac{4m_l^2}{q^2}\right) + H^{(2)} H^{\dagger(2)} \left(1 - \frac{4m_l^2}{q^2}\right) + \frac{2m_l^2}{q^2} 3 H_t^{(2)} H_t^{\dagger(2)}} \quad (15)$$

It should be noted that the forward backward asymmetry observable  $A_{FB}(q^2)$  for the  $B_c \rightarrow D_s \mu^+ \mu^-$  decay mode is zero in the SM as the helicity amplitudes  $H_{\pm}^i = 0$ . It is worth mentioning that it can have a non zero value only if it receives contribution from scalar, pseudoscalar or tensor NP operators. Since we consider NP in vector and axial vector operators only, we do not discuss  $A_{FB}(q^2)$  for the  $B_c \rightarrow D_s \mu^+ \mu^-$  decay mode in section. IV.

## IV. RESULTS AND DISCUSSION

### A. Inputs

For definiteness, we first report all the inputs that are used for the computation of all the decay observables. We employ a renormalization scale of  $\mu = 4.8 \text{ GeV}$  throughout our analysis. For the meson masses, we use  $M_{B_c} = 6.2751 \text{ GeV}$ ,  $M_{D_s} = 1.968 \text{ GeV}$ , and  $M_{D_s^*} = 2.1122 \text{ GeV}$ , as given in Ref. [47]. For the lepton masses, we use  $m_e = 0.5109989461 \times 10^{-3} \text{ GeV}$  and  $m_\mu = 0.1056583715 \text{ GeV}$  from Ref. [47]. Similarly, the mean life time of  $B_c$  meson and the Fermi coupling constant are taken to be  $\tau_{B_c} = 0.507 \times 10^{-12} \text{ s}$  and  $G_F = 1.1663787 \times 10^{-5} \text{ GeV}^{-2}$ , as reported in Ref. [47]. For the quark masses, we use  $m_b(\overline{\text{MS}}) = 4.2 \text{ GeV}$ ,  $m_c(\overline{\text{MS}}) = 1.28 \text{ GeV}$ , and  $m_b^{\text{pole}} = 4.8 \text{ GeV}$  [48]. For the electromagnetic coupling constant, we use  $\alpha_e^{-1} = 133.28$ . We use  $|V_{tb} V_{ts}| = 0.0401 \pm 0.0010$  as given in Ref. [49]. The WCs in our numerical estimates, taken from Refs. [50], are reported in Table. I. A relativistic quark model based

$C_1$	$C_2$	$C_3$	$C_4$	$C_5$	$C_6$	$C_7^{\text{eff}}$	$C_9$	$C_{10}$
-0.248	1.107	0.011	-0.026	0.007	-0.031	-0.313	4.344	-4.669

TABLE I: Wilson coefficients evaluated at renormalization scale of  $\mu = 4.8 \text{ GeV}$  from Ref. [50].

on quasipotential approach was adopted in Ref. [36] to determine various  $B_c \rightarrow D_s$  and  $B_c \rightarrow D_s^*$  transition form factors. Various form factors at  $q^2 = 0$  and the fitted parameters  $\sigma_1$  and  $\sigma_2$ , taken from Ref. [36], are reported in Table. II. It was shown in Ref. [36] that the  $q^2$  dependence of the form factors can be well parametrized and reproduced

	$f_+$	$f_0$	$f_T$	$V$	$A_0$	$A_1$	$A_2$	$T_1$	$T_2$	$T_3$
$F_0$	0.129	0.129	0.098	0.182	0.070	0.089	0.110	0.085	0.085	0.051
$\sigma_1$	2.096	2.331	1.412	2.133	1.561	2.479	2.833	1.540	2.577	2.783
$\sigma_2$	1.147	1.666	0.048	1.183	0.192	1.686	2.167	0.248	1.859	2.170

TABLE II:  $B_c \rightarrow D_s$  and  $B_c \rightarrow D_s^*$  form factors at  $q^2 = 0$  and the fitted parameters  $\sigma_1$  and  $\sigma_2$  from Ref. [36].

in the form:

$$F(q^2) = \frac{F(0)}{\left(1 - \frac{q^2}{M^2}\right) \left(1 - \sigma_1 \frac{q^2}{M_{B_s^*}^2} + \sigma_2 \frac{q^4}{M_{B_s^*}^4}\right)} \quad (16)$$

for  $F(q^2) = f_+(q^2), f_T(q^2), V(q^2), A_0(q^2), T_1(q^2)$ . Whereas, for  $F(q^2) = f_0(q^2), A_1(q^2), A_2(q^2), T_2(q^2), T_3(q^2)$ , it can be well approximated by

$$F(q^2) = \frac{F(0)}{\left(1 - \sigma_1 \frac{q^2}{M_{B_s^*}^2} + \sigma_2 \frac{q^4}{M_{B_s^*}^4}\right)}, \quad (17)$$

where  $M = M_{B_s}$  for  $A_0(q^2)$  and  $M = M_{B_s^*}$  for all other form factors. We use  $M_{B_s} = 5.36689 \text{ GeV}$  and  $M_{B_s^*} = 5.4154 \text{ GeV}$  from Ref. [47]. The form factors describe the hadronisation of quarks and gluons: these involve QCD in the non-perturbative regime and are a significant source of theoretical uncertainties. To gauge the effect of the form factor uncertainties on various observables, we have used  $\pm 5\%$  uncertainty in  $F(0)$ ,  $\sigma_1$  and  $\sigma_2$ .

### B. SM prediction of $B_c \rightarrow (D_s, D_s^*) l \bar{l}$ decay observables

Now let us proceed to discuss our results in the SM. In Table. III, we report our  $q^2$  bin averaged values of various observables for the  $B_c \rightarrow D_s \mu^+ \mu^-$  and  $B_c \rightarrow D_s^* \mu^+ \mu^-$  decays. We restrict our analysis to low dilepton invariant mass region and consider seven  $q^2$  bins ranging from  $(0.045 - 6.0) \text{ GeV}^2$ . The central values are obtained using the central values of all the input parameters. For the uncertainties, we have performed a naive  $\chi^2$  analysis defined as

$$\chi^2 = \sum_i \frac{(\mathcal{O}_i - \mathcal{O}_i^0)^2}{\Delta_i^2}, \quad (18)$$

where  $\mathcal{O}_i = (|V_{tb}V_{ts}^*|, F(0), \sigma_1, \sigma_2)$ . Here  $\mathcal{O}_i^0$  represents the central values of all the parameters and  $\Delta_i$  represents  $1\sigma$  uncertainty associated with each parameter. To find out the uncertainties in each observable, We impose  $\chi^2 \leq 2.156$  for the  $B_c \rightarrow D_s \mu^+ \mu^-$  decays and  $\chi^2 \leq 8.643$  for the  $B_c \rightarrow D_s^* \mu^+ \mu^-$  decays. In the SM, we find the branching ratios

Observable/ $q^2$ bin	[0.045 – 1.0]	[1.0 – 2.0]	[2.0 – 3.0]	[3.0 – 4.0]	[4.0 – 5.0]	[5.0 – 6.0]	[1.0 – 6.0]
$10^7 \times \mathcal{B}(B_c \rightarrow D_s \mu \mu)$	$0.025 \pm 0.001$	$0.030 \pm 0.002$	$0.034 \pm 0.002$	$0.038 \pm 0.002$	$0.043 \pm 0.003$	$0.049 \pm 0.004$	$0.194 \pm 0.013$
$R_{D_s}$	$1.006 \pm 0.008$	$1.007 \pm 0.002$	$1.005 \pm 0.001$	$1.004 \pm 0.001$	$1.003 \pm 0.001$	$1.003 \pm 0.001$	$1.004 \pm 0.001$
$10^7 \times \mathcal{B}(B_c \rightarrow D_s^* \mu \mu)$	$0.024 \pm 0.001$	$0.011 \pm 0.001$	$0.014 \pm 0.002$	$0.020 \pm 0.002$	$0.028 \pm 0.003$	$0.039 \pm 0.004$	$0.113 \pm 0.012$
$\langle A_{FB}^{D_s^*} \rangle$	$-0.064 \pm 0.002$	$-0.076 \pm 0.012$	$0.033 \pm 0.006$	$0.110 \pm 0.009$	$0.160 \pm 0.011$	$0.194 \pm 0.013$	$0.123 \pm 0.009$
$\langle F_L^{D_s^*} \rangle$	$0.266 \pm 0.033$	$0.711 \pm 0.034$	$0.662 \pm 0.032$	$0.566 \pm 0.035$	$0.488 \pm 0.036$	$0.430 \pm 0.037$	$0.526 \pm 0.035$
$R_{D_s^*}$	$0.999 \pm 0.005$	$0.993 \pm 0.002$	$0.992 \pm 0.001$	$0.993 \pm 0.001$	$0.994 \pm 0.001$	$0.995 \pm 0.001$	$0.994 \pm 0.001$

TABLE III:  $q^2$  bin (in  $\text{GeV}^2$ ) averaged values of various observables of  $B_c \rightarrow D_s \mu^+ \mu^-$  and  $B_c \rightarrow D_s^* \mu^+ \mu^-$  decays in the SM. The uncertainties in each observable corresponds to the uncertainties associated with the meson to meson transition form factors and the CKM matrix elements.

of  $B_c \rightarrow (D_s, D_s^*) \mu^+ \mu^-$  decays to be of  $\mathcal{O}(10^{-8})$  which might be within the experimental sensitivity of LHCb because of the large number of  $B_c$  meson that is being produced at the LHC. We also obtain the LFU ratios to be  $R_{D_s, D_s^*} \approx 1$  in the SM. It is observed that in the  $q^2$  bin ranging from  $(0.045 - 2) \text{ GeV}^2$ , the  $\langle A_{FB}^{D_s^*} \rangle$  observable assumes negative values, whereas, for  $q^2 > 2 \text{ GeV}^2$ , it assumes positive values. It should be noted that the uncertainty associated with the LFU ratios  $R_{D_s}$  and  $R_{D_s^*}$  are quite negligible in comparison to the uncertainties present in the branching ratio, the forward backward asymmetry  $\langle A_{FB}^{D_s^*} \rangle$  and the longitudinal polarization fraction of the  $D_s^*$  meson  $\langle F_L^{D_s^*} \rangle$ . Measurements of these ratios in future will be crucial in determining various NP Lorentz structures.

We have shown in Fig. 1 the  $q^2$  dependence of differential branching ratios, forward backward asymmetry, and longitudinal polarization fraction of  $D_s^*$  meson in the low  $q^2$  region  $0.045 \leq q^2 \leq 6 \text{ GeV}^2$ . The line corresponds to the central values of all the input parameters, whereas, the band corresponds to the uncertainties associated with the CKM matrix element and the form factor inputs. In the SM, we find the zero crossing in  $A_{FB}(q^2)$  of  $B_c \rightarrow D_s^* \mu^+ \mu^-$  decays at  $q^2 = 2.2 \text{ GeV}^2$ . Our results are quite similar to the values reported in Ref. [36]. Slight deviations may occur due to different choices of input parameters.

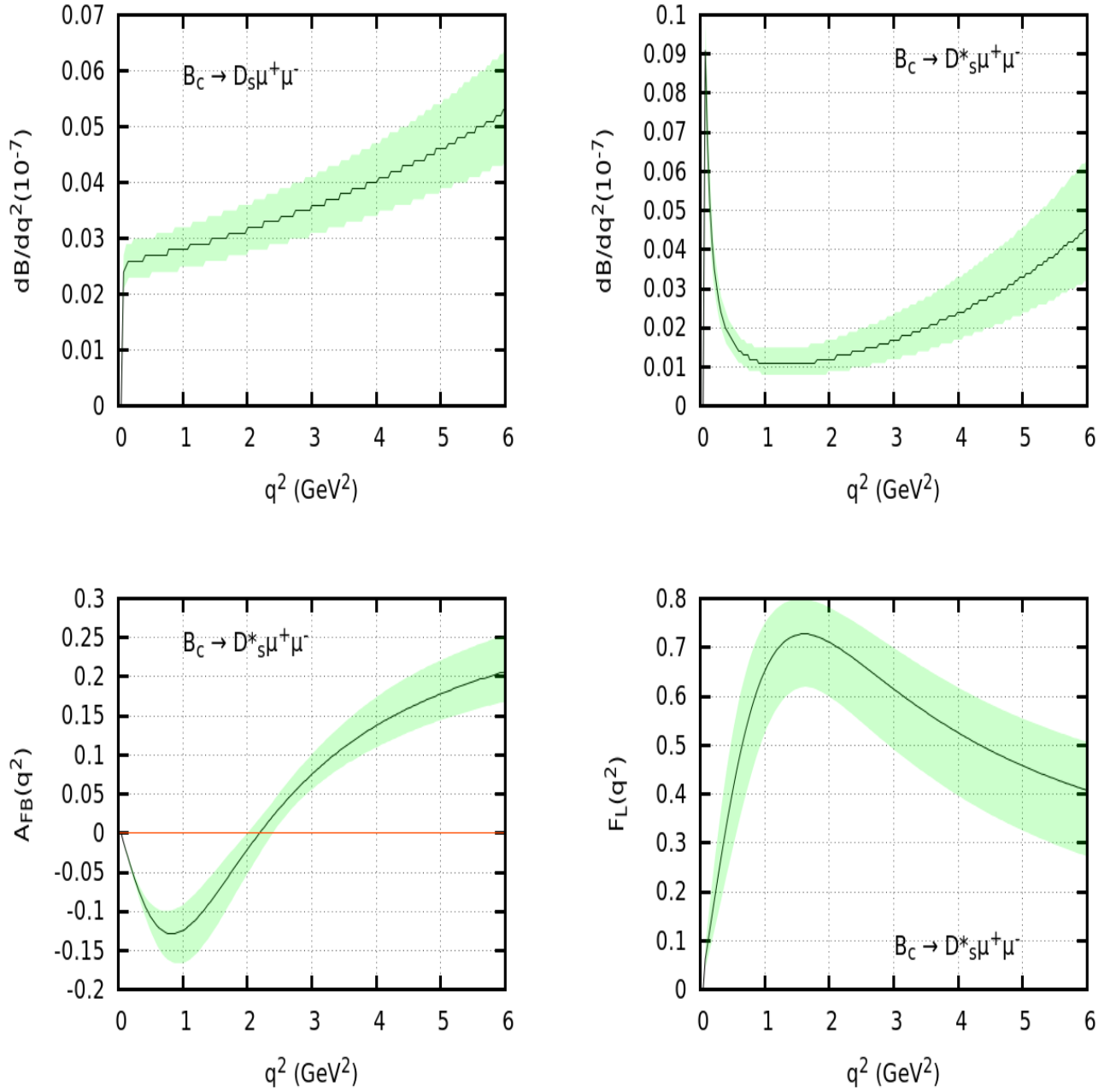


FIG. 1: Differential branching ratio  $d\mathcal{B}/dq^2$ , forward backward asymmetry of lepton pair  $A_{FB}(q^2)$  and longitudinal polarization fraction of  $D_s^*$  meson  $F_L(q^2)$  for the  $B_c \rightarrow D_s \mu^+ \mu^-$  and  $B_c \rightarrow D_s^* \mu^+ \mu^-$  decays in the SM. The band corresponds to the uncertainties in the transition form factors and the CKM matrix elements as discussed in the text.

### C. New Physics analysis

Our main objective is to determine the effect of NP on  $B_c \rightarrow (D_s, D_s^*) \mu^+ \mu^-$  decay observables in a model independent way. To this end, we use an effective theory formalism in the presence of new vector (V) and axial vector (A) couplings in our analysis. Although there can be other NP Lorentz structures such as scalar (S), pseudoscalar (P) and tensor (T), they are severely constrained by  $B_s \rightarrow \mu\mu$  and  $b \rightarrow s\gamma$  data. Hence we omit any discussion regarding these NP operators. Global fits of NP to the  $b \rightarrow s l^+ l^-$  data have been carried out by several groups [21–30]. In Ref. [30],

the authors perform a global fit of  $C_9^{NP}$ ,  $C_{10}^{NP}$ ,  $C'_9$ , and  $C'_{10}$  by using the constraints coming not only from  $R_K$ ,  $R_{K^*}$ ,  $P'_5$ , and  $\mathcal{B}(B_s \rightarrow \phi \mu^+ \mu^-)$  but also from  $\mathcal{B}(B_s \rightarrow \mu^+ \mu^-)$ , differential branching ratios of  $B^{0,+} \rightarrow K^{0,+*} \mu^+ \mu^-$ ,  $B^{0,+} \rightarrow K^{0,+} \mu^+ \mu^-$  and  $B \rightarrow X_s \mu^+ \mu^-$ , angular observables in  $B^0 \rightarrow K^{0*} \mu^+ \mu^-$  and  $B_s \rightarrow \phi \mu^+ \mu^-$  decays. Two different scenarios were considered in Ref. [30]. In 1D scenario, the best solutions to these anomalies were obtained for  $C_9^{NP}$ ,  $C_{10}^{NP}$ ,  $C_9^{NP} = -C_{10}^{NP}$  and  $C_9^{NP} = -C'_9$ . Similarly, for 2D scenario, where NP contributes to two WCs, the best solutions were obtained for  $(C_9^{NP}, C_{10}^{NP})$ ,  $(C_9^{NP}, C'_9)$ , and  $(C_9^{NP}, C'_{10})$ . There are other possibilities with different WCs exist that give rise to similar fits. We, however, consider only seven of them: four from 1D scenario and three from 2D scenario. The best fit values and the corresponding  $\Delta\chi^2$  values of all these NP WCs for 1D and 2D scenarios, taken from Ref. [30], are reported in Table. IV. It should be noted that NP contributions to  $(C_9^{NP}, C'_9)$  and  $(C_9^{NP}, C'_{10})$  are the most favored ones from the 2D scenario and NP in  $C_9^{NP} = -C'_9$  is the most favored one from 1D scenario.

Wilson coefficients	Best fit values	$\Delta\chi^2$
$C_9^{NP}$	-1.07	37.6
$C_{10}^{NP}$	+0.78	27.0
$C_9^{NP} = -C_{10}^{NP}$	-0.52	36.3
$C_9^{NP} = -C'_9$	-1.11	40.5
$(C_9^{NP}, C_{10}^{NP})$	(-0.94, +0.23)	41.8
$(C_9^{NP}, C'_9)$	(-1.27, +0.68)	49.4
$(C_9^{NP}, C'_{10})$	(-1.36, -0.46)	52.8

TABLE IV: Best fit and the corresponding  $\Delta\chi^2$  values of different new vector and axial vector Wilson coefficients in 1D and 2D scenarios taken from Ref. [30].

In Appendix , we report  $q^2$  bin averaged values of various observables such as the branching ratio, ratio of branching ratio, forward backward asymmetry, and longitudinal polarization fraction of the  $D_s^*$  meson for the  $B_c \rightarrow D_s \mu^+ \mu^-$  and  $B_c \rightarrow D_s^* \mu^+ \mu^-$  decays in the presence of these NP WCs. In each  $q^2$  bin, the branching ratio of  $B_c \rightarrow D_s \mu^+ \mu^-$  is smaller in each NP scenarios than in the SM except for  $C_9^{NP} = -C'_9$ . It remains SM like for  $C_9^{NP} = -C'_9$ . Similar conclusion can be made for the ratio of branching ratio  $R_{D_s}$  as well. For the  $B_c \rightarrow D_s^* \mu^+ \mu^-$  decay, the bin averaged branching ratio and the ratio of branching ratio  $R_{D_s^*}$  in each  $q^2$  bin for each NP scenarios are smaller than the corresponding SM value. However, the  $A_{FB}$  and  $F_L$  values can be either smaller or larger in NP cases than the SM central value. It should be mentioned that the deviation of  $R_{D_s}$ ,  $R_{D_s^*}$  and  $A_{FB}$  from the SM prediction can be quite large in some  $q^2$  bins.

In Fig. 2, we show various  $q^2$  dependent observables for the  $B_c \rightarrow (D_s, D_s^*) \mu^+ \mu^-$  decays in the presence of various NP WCs in 1D scenario. Our observations are as follows:

- The differential branching ratio for the  $B_c \rightarrow D_s \mu^+ \mu^-$  decays is reduced at all  $q^2$  for  $C_9^{NP}$ ,  $C_{10}^{NP}$ , and  $C_9^{NP} = -C_{10}^{NP}$ , whereas, it remains SM like for  $C_9^{NP} = -C'_9$ . This could very well be understood from Eq. 8 that  $H_0^{(1)}$  and  $H_t^{(1)}$  helicity amplitudes for the  $B_c \rightarrow D_s \mu^+ \mu^-$  decay mode depend on the combination  $C_9^{NP} + C'_9$ . Hence the NP contribution cancels.
- The differential branching ratio for the  $B_c \rightarrow D_s^* \mu^+ \mu^-$  decays is reduced at all  $q^2$  for  $C_9^{NP}$ ,  $C_{10}^{NP}$ ,  $C_9^{NP} = -C_{10}^{NP}$ , and  $C_9^{NP} = -C'_9$ . The deviation with the SM prediction increases as  $q^2$  increases for each NP WCs.
- For all the NP couplings, the zero crossing in the forward backward asymmetry observable  $A_{FB}^{D_s^*}$  is shifted to the higher values of  $q^2$  than in the SM. There is, however, one exception. For  $C_{10}^{NP} = 0.78$ , the zero crossing coincides with the SM prediction although the shape of  $A_{FB}^{D_s^*}$  may slightly vary. Maximum deviation from the SM prediction is observed for  $C_9^{NP}$  and  $C_9^{NP} = -C'_9$ .
- The peak of the longitudinal polarization fraction of  $D_s^*$  meson may shift towards a higher values of  $q^2$  than in the SM. Although the longitudinal polarization fraction  $F_L$  is reduced at all  $q^2$  for  $C_9^{NP}$ ,  $C_9^{NP} = -C_{10}^{NP}$ , and  $C_9^{NP} = -C'_9$ , it may increase with  $C_{10}^{NP}$  for  $q^2 > 1.2 \text{ GeV}^2$ .

There are other combinations of VA couplings exist in the 1D scenario as reported in Ref. [30]. We, however, do not consider those cases because of their small  $\Delta\chi^2$  values.



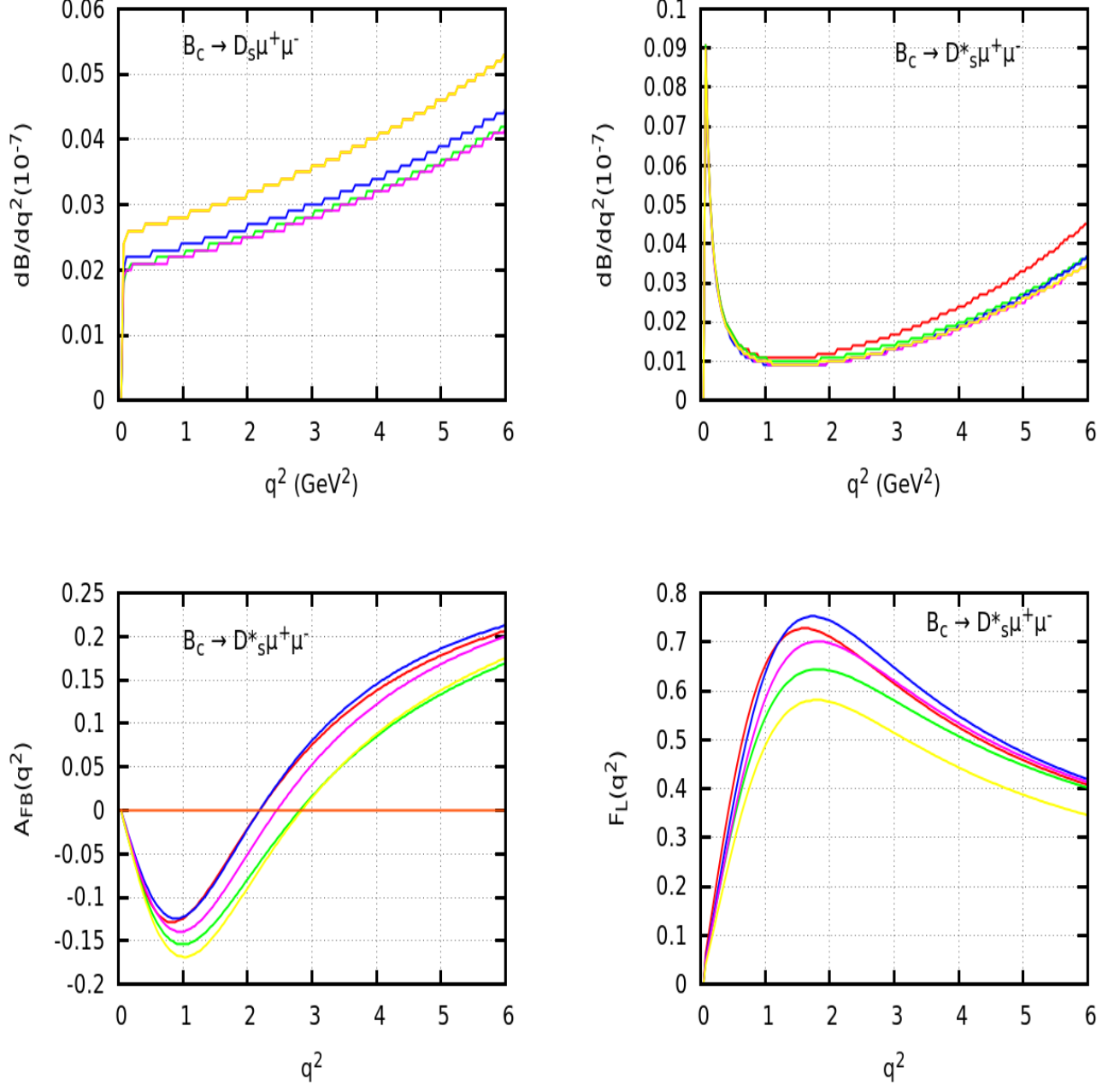


FIG. 2: Differential branching ratio  $dB/dq^2$ , forward backward asymmetry of lepton pair  $A_{FB}(q^2)$  and longitudinal polarization fraction of  $D_s^*$  meson  $F_L(q^2)$  for the  $B_c \rightarrow D_s \mu^+ \mu^-$  and  $B_c \rightarrow D_s^* \mu^+ \mu^-$  decays in the SM (Red) and for the best fit values of new VA couplings in 1D scenario. Green, blue, purple, and yellow lines correspond to the best fit values of  $C_9^{NP} = -1.07$ ,  $C_{10}^{NP} = 0.78$ ,  $C_9^{NP} = -C_{10}^{NP} = -0.52$ , and  $C_9^{NP} = -C_9' = -1.11$ , respectively.

We now consider several NP couplings from the 2D scenarios having high  $\Delta\chi^2$  values from the global fit [30]. The best fit values, taken from Ref. [30], are reported in table. IV. We show in Fig. 3 various observables such as Differential branching ratio  $dB/dq^2$ , forward backward asymmetry of lepton pair  $A_{FB}(q^2)$  and longitudinal polarization fraction of  $D_s^*$  meson  $F_L(q^2)$  as a function of dilepton invariant mass  $q^2$  for the  $B_c \rightarrow D_s \mu^+ \mu^-$  and  $B_c \rightarrow D_s^* \mu^+ \mu^-$  decays in the presence of such NP. Our main observations are as follows:

- The differential branching ratio for the  $B_c \rightarrow D_s \mu^+ \mu^-$  decay is reduced at all  $q^2$  for each NP couplings. The

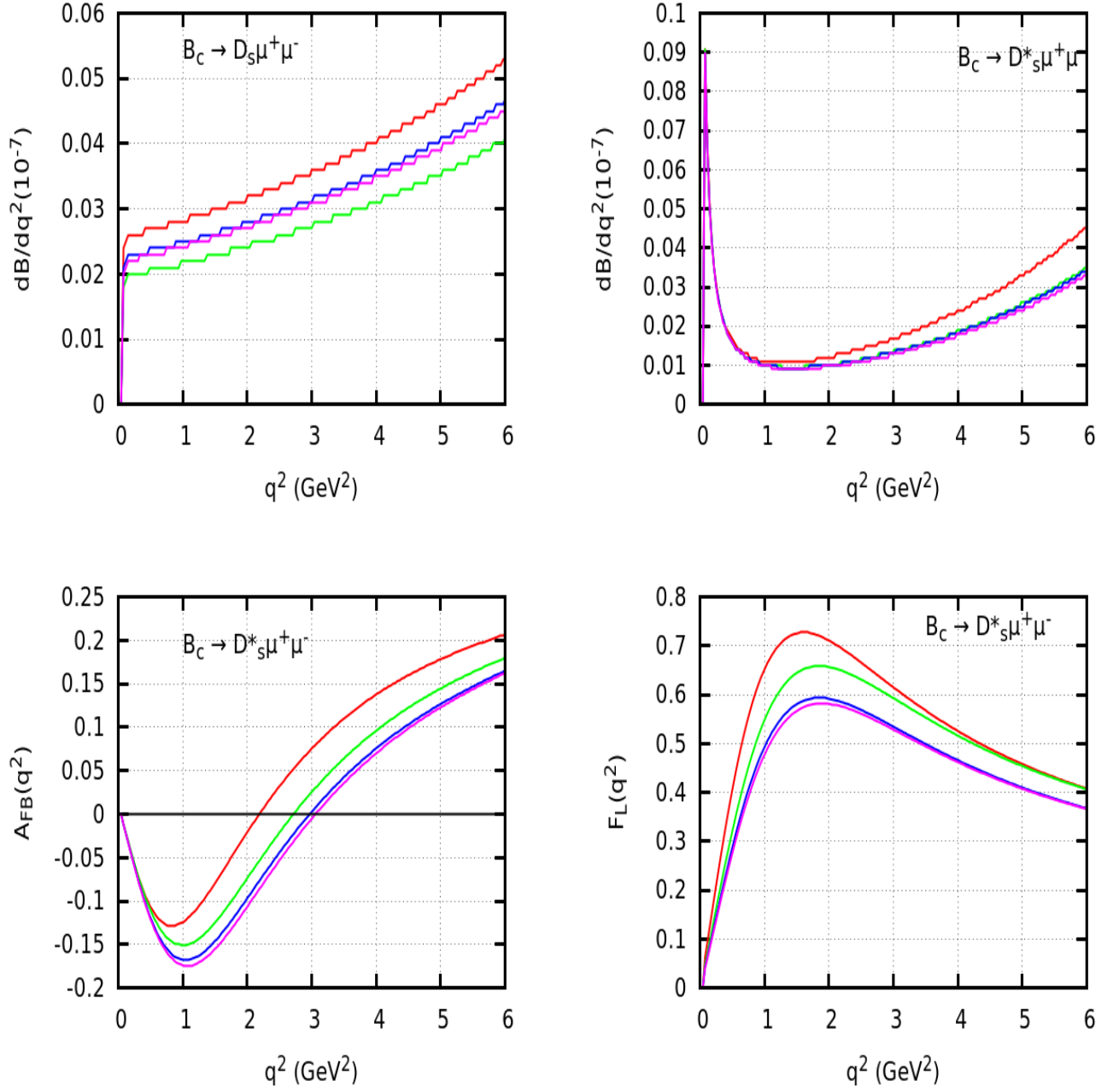


FIG. 3: Differential branching ratio  $d\mathcal{B}/dq^2$ , forward backward asymmetry of lepton pair  $A_{FB}(q^2)$  and longitudinal polarization fraction of  $D_s^*$  meson  $F_L(q^2)$  for the  $B_c \rightarrow D_s \mu^+ \mu^-$  and  $B_c \rightarrow D_s^* \mu^+ \mu^-$  decays in the SM (Red) and for the best fit values of new VA couplings in 2D scenario. Green, blue and purple lines correspond to the best fit values of  $(C_9^{NP}, C_{10}^{NP}) = (-0.94, +0.23)$ ,  $(C_9^{NP}, C_9') = (-1.27, +0.68)$  and  $(C_9^{NP}, C_{10}') = (-1.36, -0.46)$ , respectively.

deviation from the SM prediction is more pronounced in case of  $(C_9^{NP}, C_{10}^{NP}) = (-0.94, +0.23)$ .

- Similar to  $B_c \rightarrow D_s \mu^+ \mu^-$ , the differential branching ratio for the  $B_c \rightarrow D_s^* \mu^+ \mu^-$  decay also is reduced at all  $q^2$ . The deviation with the SM prediction, however, increases with increase in  $q^2$ . It reaches maximum at  $q^2 = 6 \text{ GeV}^2$ .
- The zero crossing in the forward backward asymmetry observable  $A_{FB}(q^2)$  is shifted to higher values of  $q^2$

than in the SM for each NP couplings. The maximum deviation from the SM prediction is observed for  $(C_9^{NP}, C'_{10}) = (-1.36, -0.46)$  which is shown with a purple line in Fig. 3.

- The longitudinal polarization fraction of the  $D_s^*$  meson  $F_L(q^2)$  decreases once we include the NP couplings. It is observed that the peak of the  $F_L(q^2)$  distribution reduces and shifted towards slightly higher  $q^2$  than in the SM. Maximum deviation from the SM prediction is observed for  $(C_9^{NP}, C'_{10}) = (-1.36, -0.46)$  which is shown with a purple line in Fig. 3.

## V. CONCLUSION

Motivated by the anomalies present in  $B \rightarrow (K, K^*)\mu^+\mu^-$  decays, we have analyzed  $B_c \rightarrow (D_s, D_s^*)\mu^+\mu^-$  decays mediated via  $b \rightarrow sl^+l^-$  neutral current transitions using the  $B_c \rightarrow (D_s, D_s^*)$  transition form factors obtained in the relativistic quark model. We use a model independent effective theory formalism and include NP effects coming from new vector and axial vector operators only. We discard scalar, pseudoscalar and tensor operators as they are severely constrained by  $B_s \rightarrow \mu\mu$  and  $b \rightarrow s\gamma$  data. Several authors have performed global fits to the  $b \rightarrow sl^+l^-$  data and proposed two types of NP scenarios, namely,  $1D$  and  $2D$  scenarios. In the  $1D$  scenario, we chose four NP scenarios in which the NP contribution is coming from only one NP WCs at a time. In the  $2D$  scenario, we chose three NP scenarios in which the NP contribution is coming from two NP WCs at a time.

We give predictions on several observables such as branching ratio, ratio of branching ratio, forward backward asymmetry, and the longitudinal polarization fraction of the  $D_s^*$  meson in the SM and in several NP cases. We observe that for most of the NP cases, the branching ratio for both the decay modes is reduced at all  $q^2$ . In most cases, the zero of  $A_{FB}(q^2)$  parameter is shifted to the higher value of  $q^2$  than in the SM. However, with only  $C_{10}^{NP}$ , the zero crossing is SM like. Similarly, for the longitudinal polarization fraction of the  $D_s^*$  meson, the peak of the distribution is reduced at all  $q^2$  and it is slightly shifted towards higher value of  $q^2$  than in the SM.

Although there is hint of NP in  $b \rightarrow sl^+l^-$  transition decays, NP is not yet established. Unlike  $B \rightarrow (K, K^*)\mu^+\mu^-$  decays which are rigorously studied both theoretically and experimentally, the  $B_c \rightarrow (D_s, D_s^*)\mu^+\mu^-$  decays mediated via same  $b \rightarrow sl^+l^-$  neutral current transitions received very less attention. Measurement of various observables for the  $B_c \rightarrow (D_s, D_s^*)\mu^+\mu^-$  decays and at the same time improved estimates of various  $B_c \rightarrow D_s$  and  $B_c \rightarrow D_s^*$  transition form factors in future will be crucial in identifying the true nature of NP. Again, to enhance the significance of various measurements related to  $b \rightarrow sl^+l^-$  decays and to disentangle genuine NP effects from various statistical and systematic uncertainties, more data samples are needed.

## Appendix

Here we report the  $q^2$  bin averaged values of all the observables for the  $B_c \rightarrow (D_s, D_s^*)\mu^+\mu^-$  decays in the SM and in several NP cases.

$q^2$ bin (GeV <sup>2</sup> )	SM	$C_9^{NP}$	$C_{10}^{NP}$	$C_9^{NP} = -C_{10}^{NP}$	$C_9^{NP} = -C'_9$	$(C_9^{NP}, C_{10}^{NP})$	$(C_9^{NP}, C'_9)$	$(C_9^{NP}, C'_{10})$
[0.045, 1.0]	0.025	0.020	0.021	0.020	0.025	0.019	0.022	0.022
[1.0, 2.0]	0.030	0.024	0.025	0.023	0.030	0.023	0.026	0.026
[2.0, 3.0]	0.034	0.027	0.028	0.026	0.034	0.026	0.030	0.029
[3.0, 4.0]	0.038	0.030	0.032	0.030	0.038	0.029	0.033	0.033
[4.0, 5.0]	0.043	0.034	0.036	0.034	0.043	0.033	0.038	0.037
[5.0, 6.0]	0.049	0.039	0.042	0.039	0.049	0.038	0.043	0.042
[1.0, 6.0]	0.193	0.154	0.163	0.152	0.193	0.149	0.171	0.166

TABLE V:  $q^2$  bin averaged values of  $10^7 \times \mathcal{B}(B_c \rightarrow D_s\mu^+\mu^-)$  in the SM and in several NP cases from  $1D$  and  $2D$  scenarios.

$q^2$ bin (GeV <sup>2</sup> )	SM	$C_9^{NP}$	$C_{10}^{NP}$	$C_9^{NP} = -C_{10}^{NP}$	$C_9^{NP} = -C'_9$	$(C_9^{NP}, C_{10}^{NP})$	$(C_9^{NP}, C'_9)$	$(C_9^{NP}, C'_{10})$
[0.045, 1.0]	1.006	0.798	0.846	0.788	1.006	0.770	0.884	0.859
[1.0, 2.0]	1.007	0.803	0.845	0.790	1.007	0.774	0.888	0.867
[2.0, 3.0]	1.005	0.802	0.844	0.788	1.005	0.773	0.886	0.865
[3.0, 4.0]	1.004	0.801	0.844	0.788	1.004	0.772	0.885	0.863
[4.0, 5.0]	1.003	0.800	0.845	0.789	1.003	0.772	0.884	0.861
[5.0, 6.0]	1.003	0.799	0.847	0.790	1.003	0.772	0.884	0.859
[1.0, 6.0]	1.004	0.801	0.845	0.789	1.004	0.773	0.885	0.863

TABLE VI:  $q^2$  bin averaged values of  $R_{D_s}$  in the SM and in several NP cases from  $1D$  and  $2D$  scenarios.

$q^2$ bin (GeV <sup>2</sup> )	SM	$C_9^{NP}$	$C_{10}^{NP}$	$C_9^{NP} = -C_{10}^{NP}$	$C_9^{NP} = -C'_9$	$(C_9^{NP}, C_{10}^{NP})$	$(C_9^{NP}, C'_9)$	$(C_9^{NP}, C'_{10})$
[0.045, 1.0]	0.024	0.024	0.023	0.023	0.023	0.023	0.023	0.023
[1.0, 2.0]	0.011	0.010	0.009	0.009	0.009	0.010	0.010	0.009
[2.0, 3.0]	0.014	0.012	0.011	0.011	0.011	0.012	0.011	0.011
[3.0, 4.0]	0.020	0.017	0.016	0.015	0.016	0.016	0.016	0.015
[4.0, 5.0]	0.028	0.023	0.022	0.022	0.022	0.022	0.022	0.021
[5.0, 6.0]	0.039	0.032	0.031	0.030	0.030	0.030	0.030	0.028
[1.0, 6.0]	0.113	0.095	0.090	0.087	0.088	0.089	0.088	0.085

TABLE VII:  $q^2$  bin averaged values of  $10^7 \times \mathcal{B}(B_c \rightarrow D_s^* \mu^+ \mu^-)$  in the SM and in several NP cases from  $1D$  and  $2D$  scenarios.

$q^2$ bin (GeV <sup>2</sup> )	SM	$C_9^{NP}$	$C_{10}^{NP}$	$C_9^{NP} = -C_{10}^{NP}$	$C_9^{NP} = -C'_9$	$(C_9^{NP}, C_{10}^{NP})$	$(C_9^{NP}, C'_9)$	$(C_9^{NP}, C'_{10})$
[0.045, 1.0]	0.999	0.995	0.994	0.957	0.961	0.977	0.975	0.970
[1.0, 2.0]	0.993	0.915	0.801	0.815	0.834	0.860	0.855	0.830
[2.0, 3.0]	0.992	0.859	0.776	0.770	0.790	0.804	0.797	0.767
[3.0, 4.0]	0.993	0.834	0.781	0.760	0.778	0.783	0.774	0.744
[4.0, 5.0]	0.994	0.820	0.790	0.760	0.772	0.774	0.763	0.733
[5.0, 6.0]	0.995	0.812	0.799	0.763	0.768	0.769	0.756	0.726
[1.0, 6.0]	0.994	0.834	0.791	0.768	0.786	0.786	0.776	0.746

TABLE VIII:  $q^2$  bin averaged values of  $R_{D_s^*}$  in the SM and in several NP cases from  $1D$  and  $2D$  scenarios.

$q^2$ bin (GeV <sup>2</sup> )	SM	$C_9^{NP}$	$C_{10}^{NP}$	$C_9^{NP} = -C_{10}^{NP}$	$C_9^{NP} = -C'_9$	$(C_9^{NP}, C_{10}^{NP})$	$(C_9^{NP}, C'_9)$	$(C_9^{NP}, C'_{10})$
[0.045, 1.0]	-0.064	-0.069	-0.056	-0.062	-0.072	-0.066	-0.072	-0.072
[1.0, 2.0]	-0.076	-0.124	-0.079	-0.103	-0.138	-0.121	-0.141	-0.150
[2.0, 3.0]	0.033	-0.028	0.035	0.006	-0.033	-0.020	-0.043	-0.052
[3.0, 4.0]	0.110	0.055	0.117	0.092	0.055	0.065	0.043	0.037
[4.0, 5.0]	0.160	0.112	0.168	0.148	0.116	0.123	0.104	0.099
[5.0, 6.0]	0.194	0.153	0.201	0.186	0.159	0.164	0.147	0.144
[1.0, 6.0]	0.123	0.072	0.129	0.107	0.074	0.082	0.062	0.056

TABLE IX:  $q^2$  bin averaged values of  $\langle A_{FB}^{D_s^*} \rangle$  in the SM and in several NP cases from  $1D$  and  $2D$  scenarios.

$q^2$ bin (GeV <sup>2</sup> )	SM	$C_9^{NP}$	$C_{10}^{NP}$	$C_9^{NP} = -C_{10}^{NP}$	$C_9^{NP} = -C_9'$	$(C_9^{NP}, C_{10}^{NP})$	$(C_9^{NP}, C_9')$	$(C_9^{NP}, C_{10}')$
[0.045, 1.0]	0.266	0.213	0.232	0.215	0.181	0.208	0.186	0.177
[1.0, 2.0]	0.711	0.620	0.725	0.671	0.558	0.630	0.567	0.554
[2.0, 3.0]	0.662	0.613	0.697	0.661	0.548	0.627	0.566	0.558
[3.0, 4.0]	0.566	0.541	0.594	0.573	0.476	0.552	0.498	0.493
[4.0, 5.0]	0.488	0.475	0.508	0.496	0.413	0.482	0.435	0.432
[5.0, 6.0]	0.430	0.423	0.444	0.437	0.365	0.428	0.387	0.385
[1.0, 6.0]	0.526	0.503	0.546	0.529	0.440	0.511	0.461	0.457

TABLE X:  $q^2$  bin averaged values of  $\langle F_L^{D^*s} \rangle$  in the SM and in several NP cases from 1D and 2D scenarios.

- 
- [1] R. Aaij *et al.* [LHCb Collaboration], “Test of lepton universality using  $B^+ \rightarrow K^+ \ell^+ \ell^-$  decays,” Phys. Rev. Lett. **113**, 151601 (2014) doi:10.1103/PhysRevLett.113.151601 [arXiv:1406.6482 [hep-ex]].
- [2] G. Hiller and F. Kruger, “More model-independent analysis of  $b \rightarrow s$  processes,” Phys. Rev. D **69**, 074020 (2004) doi:10.1103/PhysRevD.69.074020 [hep-ph/0310219].
- [3] C. Bobeth, G. Hiller and G. Piranishvili, “Angular distributions of  $\bar{B} \rightarrow \bar{K} \ell^+ \ell^-$  decays,” JHEP **0712**, 040 (2007) doi:10.1088/1126-6708/2007/12/040 [arXiv:0709.4174 [hep-ph]].
- [4] M. Bordone, G. Isidori and A. Pattori, “On the Standard Model predictions for  $R_K$  and  $R_{K^*}$ ,” Eur. Phys. J. C **76** (2016) no.8, 440 doi:10.1140/epjc/s10052-016-4274-7 [arXiv:1605.07633 [hep-ph]].
- [5] R. Aaij *et al.* [LHCb Collaboration], “Search for lepton-universality violation in  $B^+ \rightarrow K^+ \ell^+ \ell^-$  decays,” Phys. Rev. Lett. **122**, no. 19, 191801 (2019) doi:10.1103/PhysRevLett.122.191801 [arXiv:1903.09252 [hep-ex]].
- [6] R. Aaij *et al.* [LHCb Collaboration], “Test of lepton universality with  $B^0 \rightarrow K^{*0} \ell^+ \ell^-$  decays,” JHEP **1708**, 055 (2017) doi:10.1007/JHEP08(2017)055 [arXiv:1705.05802 [hep-ex]].
- [7] B. Capdevila, S. Descotes-Genon, J. Matias and J. Virto, “Assessing lepton-flavour non-universality from  $B \rightarrow K^* \ell \ell$  angular analyses,” JHEP **1610**, 075 (2016) doi:10.1007/JHEP10(2016)075 [arXiv:1605.03156 [hep-ph]].
- [8] N. Serra, R. Silva Coutinho and D. van Dyk, “Measuring the breaking of lepton flavor universality in  $B \rightarrow K^* \ell^+ \ell^-$ ,” Phys. Rev. D **95** (2017) no.3, 035029 doi:10.1103/PhysRevD.95.035029 [arXiv:1610.08761 [hep-ph]].
- [9] A. Abdesselam *et al.* [Belle Collaboration], “Test of lepton flavor universality in  $B \rightarrow K^* \ell^+ \ell^-$  decays at Belle,” arXiv:1904.02440 [hep-ex].
- [10] S. Descotes-Genon, J. Matias, M. Ramon and J. Virto, “Implications from clean observables for the binned analysis of  $B^- \rightarrow K^* \mu^+ \mu^-$  at large recoil,” JHEP **1301**, 048 (2013) doi:10.1007/JHEP01(2013)048 [arXiv:1207.2753 [hep-ph]].
- [11] S. Descotes-Genon, T. Hurth, J. Matias and J. Virto, “Optimizing the basis of  $B \rightarrow K^* \ell \ell$  observables in the full kinematic range,” JHEP **1305**, 137 (2013) doi:10.1007/JHEP05(2013)137 [arXiv:1303.5794 [hep-ph]].
- [12] R. Aaij *et al.* [LHCb Collaboration], “Measurement of Form-Factor-Independent Observables in the Decay  $B^0 \rightarrow K^{*0} \mu^+ \mu^-$ ,” Phys. Rev. Lett. **111** (2013) 191801 doi:10.1103/PhysRevLett.111.191801 [arXiv:1308.1707 [hep-ex]].
- [13] R. Aaij *et al.* [LHCb Collaboration], “Angular analysis of the  $B^0 \rightarrow K^{*0} \mu^+ \mu^-$  decay using 3 fb<sup>-1</sup> of integrated luminosity,” JHEP **1602**, 104 (2016) doi:10.1007/JHEP02(2016)104 [arXiv:1512.04442 [hep-ex]].
- [14] M. Aaboud *et al.* [ATLAS Collaboration], “Angular analysis and differential branching fraction of  $B_d^0 \rightarrow K^{*0} \mu^+ \mu^-$  decays in  $pp$  collisions at  $\sqrt{s} = 8$  TeV with the ATLAS detector,” JHEP **1810**, 047 (2018) doi:10.1007/JHEP10(2018)047 [arXiv:1805.04000 [hep-ex]].
- [15] J. Aebischer, J. Kumar, P. Stangl and D. M. Straub, “A Global Likelihood for Precision Constraints and Flavour Anomalies,” arXiv:1810.07698 [hep-ph].
- [16] A. Abdesselam *et al.* [Belle Collaboration], “Angular analysis of  $B^0 \rightarrow K^*(892)^0 \ell^+ \ell^-$ ,” arXiv:1604.04042 [hep-ex].
- [17] CMS Collaboration [CMS Collaboration], “Measurement of the  $P_1$  and  $P_2'$  angular parameters of the decay  $B^0 \rightarrow K^{*0} \mu^+ \mu^-$  in proton-proton collisions at  $\sqrt{s} = 8$  TeV,” CMS-PAS-BPH-15-008.
- [18] R. Aaij *et al.* [LHCb Collaboration], “Differential branching fraction and angular analysis of the decay  $B_s^0 \rightarrow \phi \mu^+ \mu^-$ ,” JHEP **1307**, 084 (2013) doi:10.1007/JHEP07(2013)084 [arXiv:1305.2168 [hep-ex]].
- [19] R. Aaij *et al.* [LHCb Collaboration], “Angular analysis and differential branching fraction of the decay  $B_s^0 \rightarrow \phi \mu^+ \mu^-$ ,” JHEP **1509**, 179 (2015) doi:10.1007/JHEP09(2015)179 [arXiv:1506.08777 [hep-ex]].
- [20] A. Bharucha, D. M. Straub and R. Zwicky, “ $B \rightarrow V \ell^+ \ell^-$  in the Standard Model from light-cone sum rules,” JHEP **1608**, 098 (2016) doi:10.1007/JHEP08(2016)098 [arXiv:1503.05534 [hep-ph]].
- [21] B. Capdevila, A. Crivellin, S. Descotes-Genon, J. Matias and J. Virto, “Patterns of New Physics in  $b \rightarrow s \ell^+ \ell^-$  transitions in the light of recent data,” JHEP **1801**, 093 (2018) doi:10.1007/JHEP01(2018)093 [arXiv:1704.05340 [hep-ph]].
- [22] W. Altmannshofer, P. Stangl and D. M. Straub, “Interpreting Hints for Lepton Flavor Universality Violation,” Phys. Rev. D **96**, no. 5, 055008 (2017) doi:10.1103/PhysRevD.96.055008 [arXiv:1704.05435 [hep-ph]].
- [23] G. D’Amico, M. Nardecchia, P. Panci, F. Sannino, A. Strumia, R. Torre and A. Urbano, “Flavour anomalies after the  $R_{K^*}$

- measurement,” JHEP **1709**, 010 (2017) doi:10.1007/JHEP09(2017)010 [arXiv:1704.05438 [hep-ph]].
- [24] G. Hiller and I. Nisandzic, “ $R_K$  and  $R_{K^*}$  beyond the standard model,” Phys. Rev. D **96**, no. 3, 035003 (2017) doi:10.1103/PhysRevD.96.035003 [arXiv:1704.05444 [hep-ph]].
- [25] L. S. Geng, B. Grinstein, S. Jger, J. Martin Camalich, X. L. Ren and R. X. Shi, “Towards the discovery of new physics with lepton-universality ratios of  $b \rightarrow s\ell\ell$  decays,” Phys. Rev. D **96**, no. 9, 093006 (2017) doi:10.1103/PhysRevD.96.093006 [arXiv:1704.05446 [hep-ph]].
- [26] M. Ciuchini, A. M. Coutinho, M. Fedele, E. Franco, A. Paul, L. Silvestrini and M. Valli, “On Flavourful Easter eggs for New Physics hunger and Lepton Flavour Universality violation,” Eur. Phys. J. C **77**, no. 10, 688 (2017) doi:10.1140/epjc/s10052-017-5270-2 [arXiv:1704.05447 [hep-ph]].
- [27] A. Celis, J. Fuentes-Martin, A. Vicente and J. Virto, “Gauge-invariant implications of the LHCb measurements on lepton-flavor nonuniversality,” Phys. Rev. D **96**, no. 3, 035026 (2017) doi:10.1103/PhysRevD.96.035026 [arXiv:1704.05672 [hep-ph]].
- [28] A. K. Alok, B. Bhattacharya, A. Datta, D. Kumar, J. Kumar and D. London, “New Physics in  $b \rightarrow s\mu^+\mu^-$  after the Measurement of  $R_{K^*}$ ,” Phys. Rev. D **96**, no. 9, 095009 (2017) doi:10.1103/PhysRevD.96.095009 [arXiv:1704.07397 [hep-ph]].
- [29] A. K. Alok, B. Bhattacharya, D. Kumar, J. Kumar, D. London and S. U. Sankar, “New physics in  $b \rightarrow s\mu^+\mu^-$ : Distinguishing models through CP-violating effects,” Phys. Rev. D **96**, no. 1, 015034 (2017) doi:10.1103/PhysRevD.96.015034 [arXiv:1703.09247 [hep-ph]].
- [30] A. K. Alok, A. Dighe, S. Gangal and D. Kumar, “Continuing search for new physics in  $b \rightarrow s\mu\mu$  decays: two operators at a time,” arXiv:1903.09617 [hep-ph].
- [31] A. Faessler, T. Gutsche, M. A. Ivanov, J. G. Korner and V. E. Lyubovitskij, “The Exclusive rare decays  $B \rightarrow K(K^*) \bar{\ell}\ell$  and  $B_c \rightarrow D(D^*) \bar{\ell}\ell$  in a relativistic quark model,” Eur. Phys. J. direct **4**, no. 1, 18 (2002) doi:10.1007/s1010502c0018 [hep-ph/0205287].
- [32] C. Q. Geng, C. W. Hwang and C. C. Liu, “Study of rare  $B_c^+ \rightarrow D_{d,s} +$  lepton anti-lepton decays,” Phys. Rev. D **65**, 094037 (2002) doi:10.1103/PhysRevD.65.094037 [hep-ph/0110376].
- [33] H. M. Choi, “Light-front quark model analysis of the exclusive rare  $B_c \rightarrow D_{(s)}(\ell^+\ell^-, \nu_\ell\bar{\nu}_\ell)$  decays,” Phys. Rev. D **81**, 054003 (2010) doi:10.1103/PhysRevD.81.054003 [arXiv:1001.3432 [hep-ph]].
- [34] K. Azizi, F. Falahati, V. Bashiry and S. M. Zebarjad, “Analysis of the Rare  $B(c) \rightarrow D^*(s,d) l^+ l^-$  Decays in QCD,” Phys. Rev. D **77**, 114024 (2008) doi:10.1103/PhysRevD.77.114024 [arXiv:0806.0583 [hep-ph]].
- [35] K. Azizi and R. Khosravi, “Analysis of the rare semileptonic  $B_c \rightarrow P(D, D_s)\ell^+\ell^-/\nu\bar{\nu}$  decays within QCD sum rules,” Phys. Rev. D **78**, 036005 (2008) doi:10.1103/PhysRevD.78.036005 [arXiv:0806.0590 [hep-ph]].
- [36] D. Ebert, R. N. Faustov and V. O. Galkin, “Rare Semileptonic Decays of  $B$  and  $B_c$  Mesons in the Relativistic Quark Model,” Phys. Rev. D **82**, 034032 (2010) doi:10.1103/PhysRevD.82.034032 [arXiv:1006.4231 [hep-ph]].
- [37] A. K. Alok, A. Datta, A. Dighe, M. Duraisamy, D. Ghosh and D. London, JHEP **1111**, 121 (2011) doi:10.1007/JHEP11(2011)121 [arXiv:1008.2367 [hep-ph]].
- [38] A. K. Alok, A. Datta, A. Dighe, M. Duraisamy, D. Ghosh and D. London, JHEP **1111**, 122 (2011) doi:10.1007/JHEP11(2011)122 [arXiv:1103.5344 [hep-ph]].
- [39] D. Bardhan, P. Byakti and D. Ghosh, Phys. Lett. B **773**, 505 (2017) doi:10.1016/j.physletb.2017.08.062 [arXiv:1705.09305 [hep-ph]].
- [40] M. Beneke, T. Feldmann and D. Seidel, “Systematic approach to exclusive  $B \rightarrow V l^+ l^-$ ,  $V\gamma$  decays,” Nucl. Phys. B **612**, 25 (2001) doi:10.1016/S0550-3213(01)00366-2 [hep-ph/0106067].
- [41] M. Beneke, T. Feldmann and D. Seidel, “Exclusive radiative and electroweak  $b \rightarrow d$  and  $b \rightarrow s$  penguin decays at NLO,” Eur. Phys. J. C **41**, 173 (2005) doi:10.1140/epjc/s2005-02181-5 [hep-ph/0412400].
- [42] A. J. Buras and M. Munz, “Effective Hamiltonian for  $B \rightarrow X(s) e^+ e^-$  beyond leading logarithms in the NDR and HV schemes,” Phys. Rev. D **52**, 186 (1995) doi:10.1103/PhysRevD.52.186 [hep-ph/9501281].
- [43] J. Charles, A. Le Yaouanc, L. Oliver, O. Pene and J. C. Raynal, “Heavy to light form-factors in the heavy mass to large energy limit of QCD,” Phys. Rev. D **60**, 014001 (1999) doi:10.1103/PhysRevD.60.014001 [hep-ph/9812358].
- [44] D. Ebert, R. N. Faustov and V. O. Galkin, “Form-factors of heavy to light  $B$  decays at large recoil,” Phys. Rev. D **64**, 094022 (2001) doi:10.1103/PhysRevD.64.094022 [hep-ph/0107065].
- [45] J. G. Korner and G. A. Schuler, “Exclusive Semileptonic Heavy Meson Decays Including Lepton Mass Effects,” Z. Phys. C **46**, 93 (1990).
- [46] A. Kadeer, J. G. Korner and U. Moosbrugger, “Helicity analysis of semileptonic hyperon decays including lepton mass effects,” Eur. Phys. J. C **59**, 27 (2009) [hep-ph/0511019].
- [47] M. Tanabashi *et al.* [Particle Data Group], “Review of Particle Physics,” Phys. Rev. D **98**, no. 3, 030001 (2018). doi:10.1103/PhysRevD.98.030001
- [48] W. Altmannshofer, P. Ball, A. Bharucha, A. J. Buras, D. M. Straub and M. Wick, JHEP **0901**, 019 (2009) doi:10.1088/1126-6708/2009/01/019 [arXiv:0811.1214 [hep-ph]].
- [49] M. Bona *et al.* [UTfit Collaboration], “The Unitarity Triangle Fit in the Standard Model and Hadronic Parameters from Lattice QCD: A Reappraisal after the Measurements of  $\Delta m(s)$  and  $BR(B \rightarrow \tau \nu(\tau))$ ,” JHEP **0610**, 081 (2006) doi:10.1088/1126-6708/2006/10/081 [hep-ph/0606167].
- [50] A. Ali, P. Ball, L. T. Handoko and G. Hiller, “A Comparative study of the decays  $B \rightarrow (K, K^*)\ell^+\ell^-$  in standard model and supersymmetric theories,” Phys. Rev. D **61**, 074024 (2000) doi:10.1103/PhysRevD.61.074024 [hep-ph/9910221].